

# **XM-1, the high-resolution soft x-ray microscope at the Advanced Light Source**

<sup>1</sup>Angelic Lucero\*<sup>a</sup>, Weilun Chao<sup>a,b</sup>, Gregory Denbeaux<sup>a</sup>, Thomas Eimuller<sup>c</sup>, Peter Fischer<sup>a,c</sup>, Lewis Johnson<sup>a</sup>, Matthias Koehler<sup>c</sup>, Carolyn Larabell<sup>a</sup>, Mark Le Gros<sup>a</sup>, Deborah Yager<sup>a</sup>, David Attwood<sup>a,b</sup>

<sup>a</sup>Center for X-ray Optics, Lawrence Berkeley National Laboratory, Berkeley, CA 94720

<sup>b</sup>Dept. of Electrical Engineering and Computer Science, University of California at Berkeley, Berkeley, CA 94720

<sup>c</sup>Dept. of Physics, Univ. Würzburg, EP IV, 97074 Würzburg, Germany

## **ABSTRACT**

The XM-1 soft x-ray microscope utilizes bending-magnet radiation from the Advanced Light Source (ALS) in Berkeley, CA. This radiation is collected by a “large” (9 mm diameter) fresnel condenser zone plate (CZP) which projects light through a pinhole and illuminates the sample. The radiation transmitted through the sample is then focused and magnified by a high-precision objective micro zone plate and recorded by a soft x-ray CCD camera. Our condenser zone plate and pinhole combination serves as our adjustable monochromator for selecting the desired photon energy, giving us a  $\lambda/\Delta\lambda$  of 700. This moderate spectral resolution allows for spectroscopic imaging with XM-1, including samples of magnetic materials with contrast provided by magnetic circular dichroism. Our user-friendly software programs allow for frequent utilization of complex image processing techniques. When a single field of view (10  $\mu\text{m}$  diameter) is too small, we use an automated process for combining overlapping individual images into a larger, coherent montage image. In addition, our colleagues use a labeling technique for localizing specific proteins within cellular structure. Natural antibodies are utilized to attach dense silver and gold particles to the protein of interest. A computerized process is used after the imaging to locate the sharp increases in intensity to identify the regions of labeling.

**Keywords:** x-ray microscope, XM-1, spatial resolution, X-MCD, magnetic imaging, computer processing

## **1. INTRODUCTION**

XM-1 is a soft x-ray, high resolution, full-field transmission microscope, built and operated by the Center for X-ray Optics (CXRO) at the Lawrence Berkeley National Laboratory<sup>1</sup>. XM-1 is modeled after a conventional microscope. Figure 1 shows the layout of XM-1. The x-ray source comes from an ALS bending magnet port on beamline 6.1.2. The x-ray beam is reflected off a glancing-incidence mirror to filter out higher photon energies, yielding an operating range of 250 eV – 900 eV. The x-rays are collected by a 9-mm-diameter fresnel condenser zone plate (CZP) which projects them through a pinhole onto the sample. The radiation that passes through the sample is then imaged by a 25-nm-outer-zone-width micro zone plate (MZIP) onto a soft x-ray CCD that records the image. The digital image is then saved on our main computer. Both the CZP and the MZIP are fabricated with the Nanowriter electron beam lithography tool in the Nanofabrication Laboratory at CXRO<sup>2</sup>.

XM-1 has about a 10  $\mu\text{m}$  field of view and can acquire hundreds to thousands of images per day. Samples can be imaged up to 10  $\mu\text{m}$  thick and may be in an aqueous environment. Exposures are generally a few seconds, which can be reduced by the use of thicker MZIPs. Currently there is a trade-off between higher resolution and shorter exposures. Operation of the microscope is controlled by a computer for ease of use.

---

\* Correspondence: Email: AELucero@lbl.gov; Telephone: 510-486-4079; Fax: 510-486-4550

The images obtained with XM-1 are available for viewing almost immediately via the Internet. Using a second computer set up next to the control computer, one can view previously saved images concurrently with ongoing imaging.

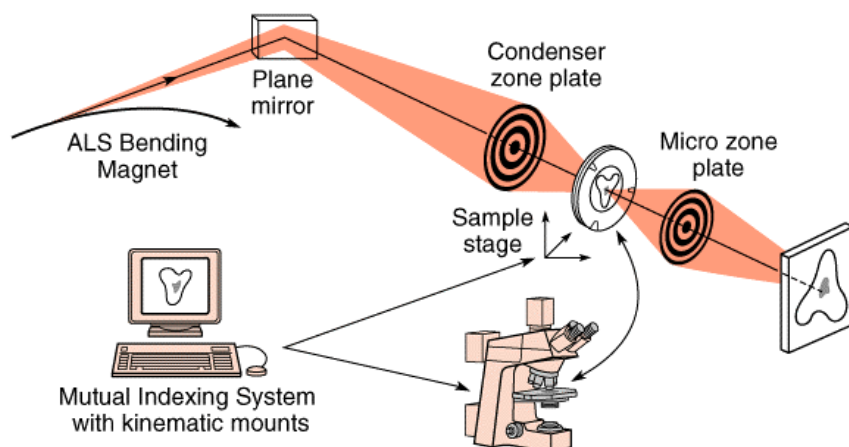


Figure 1. Optical layout of XM-1, not to scale. Zone plates are used for the condenser and objective components.

## 1.1 Spatial Resolution

We have used several test patterns comprised of small features to explore the imaging capabilities of XM-1. These tests have revealed that the spatial resolution is  $23 \text{ nm}^3$ . Figure 2 shows an x-ray image of  $15 \text{ nm}$  lines with  $60 \text{ nm}$  period and the corresponding graph of the intensity modulation.

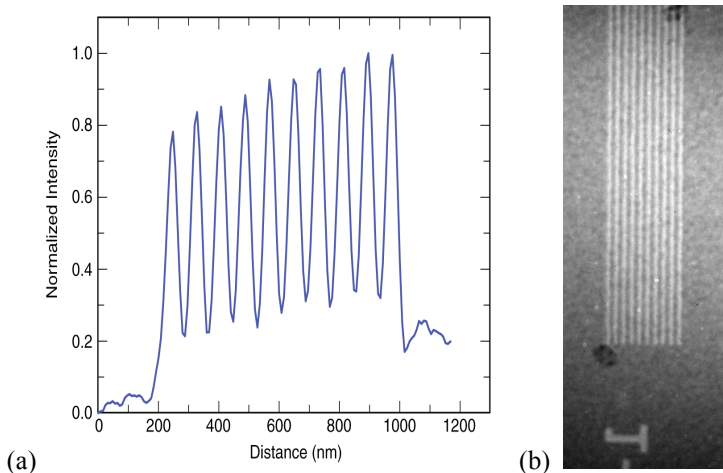


Figure 2. Line width of  $15 \text{ nm}$  with 1:3 duty cycle from a test pattern. (a) Normalized intensity plot of a line-out across pattern. (b) X-ray image of the pattern.

## 2. SPECTRAL RESOLUTION

The combination of the CZP and the pinhole acts as a linear monochromator for the microscope. Since the positions of these are variable, as well as the position of the MZP, XM-1 can be tuned to a specific wavelength to allow elemental-specific imaging and spectroscopy. We have measured the spectral resolution of XM-1 and determined that it is  $\lambda/\Delta\lambda=700$ . The measured spectrum from a sample is the convolution of the actual absorption feature of a sample with the spectrum of the instrument. In order to measure the spectral resolution of XM-1, we used the Calibration and Standards Beamline (6.3.2) at the ALS<sup>4</sup> which has a known spectral resolution of  $\lambda/\Delta\lambda>4000$  to determine very precisely the absorption of a thin sample of  $\text{CaF}_2$  at the Calcium L edge near  $350 \text{ eV}$ . Then we took the spectrum of the same sample in XM-1. With both of these measured spectra, we calculated the spectral resolution of XM-1. These three

are shown in Figure 3. It comes out to very nearly a gaussian distribution with a FWHM of 0.5 eV. Since this is at 350 eV, then the  $E/\Delta E$  or equivalently  $\lambda/\Delta\lambda=700^5$ .

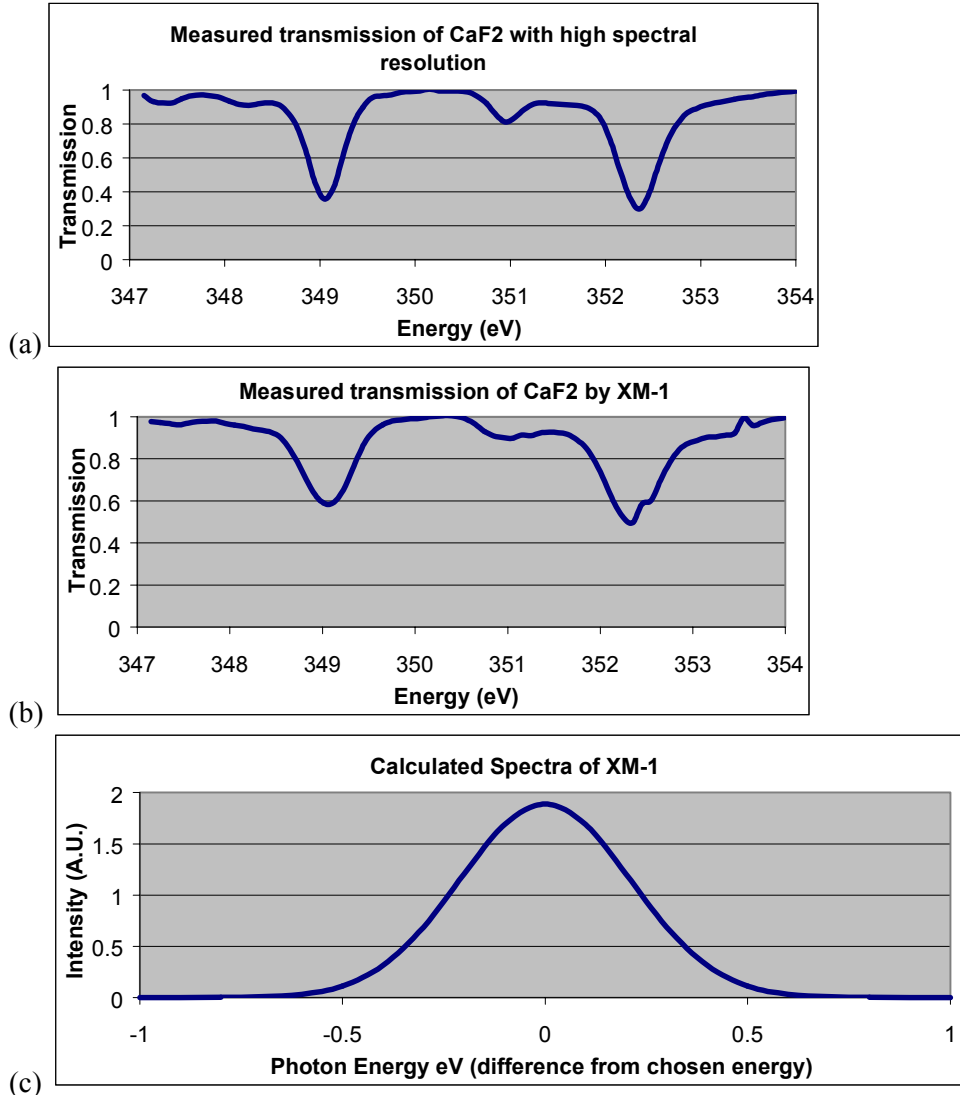


Figure 3. The measured spectrum from a sample is the convolution of the actual absorption feature of a sample with the spectrum of the instrument. The gaussian spectra of XM-1 has a FWHM of 0.5 eV at 350 eV photon energy, yielding  $\lambda/\Delta\lambda=700$ .

### 3. MAGNETIC IMAGING

In the past year, we have been imaging magnetic materials at XM-1. X-ray magnetic circular dichroism (X-MCD) serves as the contrast mechanism when imaged with circularly polarized x-rays. We obtain circular polarization by partially masking the beam from our bending magnet source at the ALS, thus utilizing the off-axis radiation emitted about 3 mm above or below the orbit plane. X-MCD in core-level absorption detects the magnetization dependence of the x-ray absorption coefficient in the vicinity of element-specific absorption edges of circularly polarized radiation. Absorption coefficients are conveniently detected in the transmission mode by counting the incoming and transmitted photon intensities. In the absorption process of a circularly polarized photon, the spin-orbit interaction in the initial core level and angular momentum conservation causes the photoelectron to act as a spin and orbital polarized probe of the polarization properties of the unoccupied levels above the Fermi energy. Thus the (spectroscopic) X-MCD signal is related to local magnetic moments. The element specificity of X-MCD

allows for imaging a single element in a multicomponent system (Figure 4). This technique has proved to be sensitive enough to observe domains at the Co L<sub>3</sub> edge of a Tb<sub>25</sub>(Fe<sub>75</sub>Co<sub>25</sub>)<sub>75</sub> system at XM-1. This sensitivity makes it feasible to form element-specific images, even with only a few monolayers of a given element. We also have begun imaging of in-plane domains using a tilt stage, and have also formed images of magnetic samples under the influence of applied magnetic fields<sup>6</sup>.

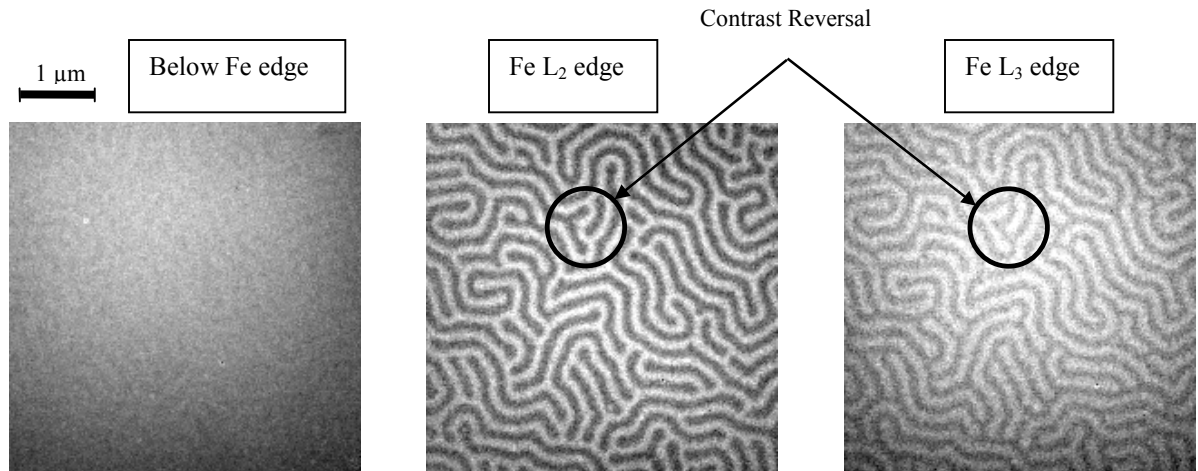


Figure 4. Images of a multilayered 75x(0.4nmGd/0.4nmFe) system. The observed change in contrast between the Fe L<sub>3</sub> and L<sub>2</sub> edges originates in the opposite spin-orbit coupling in the respective 2p<sub>3/2</sub> and 2p<sub>1/2</sub> inneratomic levels and serves as an unambiguous proof of the magnetic character of the domains observed.

#### 4. TILING

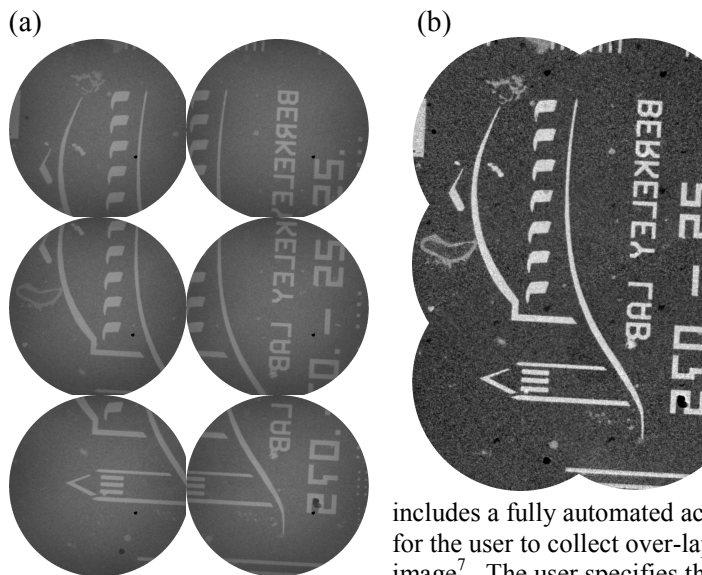


Figure 5. Images from a test pattern provided by E. Anderson. (a) Individual x-ray images. (b) The assembled montage image. Although the edges show the separate images, they are indistinguishable within the montage. Bright areas in the images show the etched out pattern.

The operation software for XM-1 includes a fully automated acquisition program, which makes it easy for the user to collect over-lapping sub-fields to form a larger area image<sup>7</sup>. The user specifies the center position, the desired over-all dimension (currently, only a square area is allowed), and the step-size between images. With the click of a button, the computer generates the required coordinates for each individual image to cover the area. A background location may also be specified along with the frequency desired for the background to be imaged. Then the computer can be activated to step through each position in the list, take an image and save that image. After the data is collected, our tiling procedure can be used to create the montage. This procedure obtains the user's choices by providing successive prompts, which makes it easy to use. This program lines up the individual images based on the stage coordinates at the time of exposure, which are



saved in each header file. Then the images are shifted and cross-correlated to line up the overlapping features, accurate on the order of our resolution limit (see Figure 5). Over-lapping areas are blended to create a smooth image.

## 5. LABELING

Often biologists are interested in the location of a specific protein throughout a cell. Knowing where the protein is located leads to information about its function. Our colleagues in the Life Sciences Department have a well-developed process for making small gold or silver particles congregate in the vicinity of a specific protein<sup>8,9</sup>. Since the gold and silver are highly absorptive, they appear as black dots within the cell. A computerized analysis of the image allows for unbiased assessment of the location of protein in the image.

### 5.1 Cell Preparation

The cell preparation involves three steps. Figure 6 illustrates the first two steps. First, chemically fixed, permeabilized cells are exposed to primary antibodies that recognize and attach to the protein of interest. Then the cells are exposed to secondary antibodies with conjugated gold particles that attach to the primary antibodies. These gold particles are 2-5 nm in diameter, which is well below our resolution limit. Subsequently, the cells are enhanced with silver to form silver aggregates around the gold of diameter on the order of the resolution of XM-1. Recently an alternate gold enhancement feature has been used. Using gold, the enhancement step is faster and gives less background enhancement relative to that with silver. The aggregate size needed is now much smaller thanks to our improved resolution.

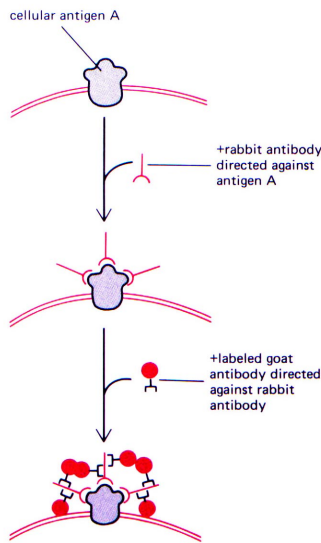


Figure 6. Primary antibodies attach first and then secondary antibodies conjugated with gold are directed against the primary antibody.

### 5.2 Computer Analysis

The silver and gold labeling absorb photons much more strongly than the rest of the cell. Thus, the area of the image that contains labeling has a dramatic decrease of photon intensity. An IDL routine is used to locate these silver or gold aggregates, based on both intensity and gradient, to create a map of the labeling within the image. This mask is superposed on the image and the color value at these points is altered to enhance the visible contrast between the labeling and the underlying cell.

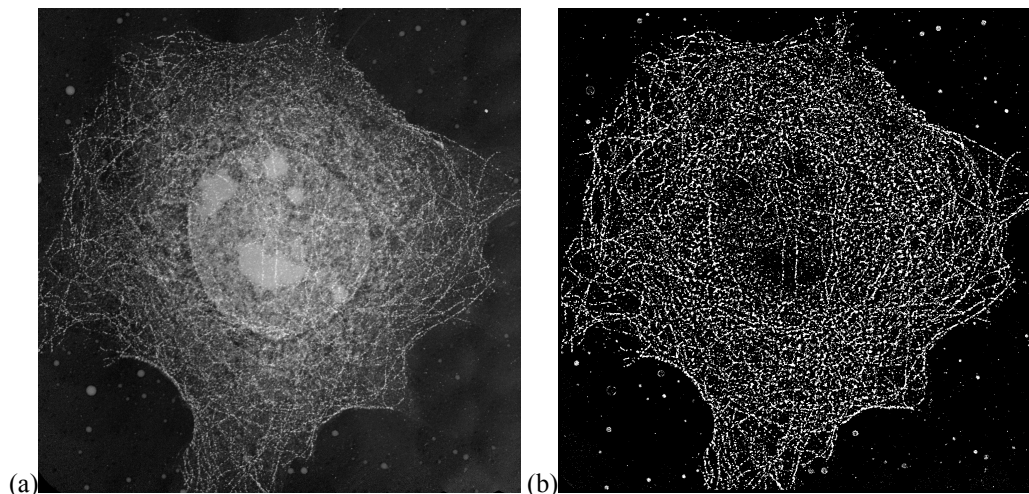


Figure 7. Montage of a hydrated mouse epithelial cell (EPH4), labeled for tubulin. The areas of highest transmission are black, while the white parts correspond to absorptive cell structure including the nucleoli clearly visible near the center. (a) Montage image of the cell with the standard gray scale. (b) The image mask of the silver aggregates as created by the IDL program. Superposition of the two images allows for determining the location of the label within the cell structure. In a colorized image, the labeling can be made visual by using a different color.

## 6. FUTURE WORK

Plans are made for continued imaging of magnetic samples, including the use of a tilted stage for imaging in-plane domains and imaging with applied magnetic fields.

We are prepared for testing zone plates of smaller outer zone width to continually improve the resolution limit of XM-1. We expect to use test patterns with smaller features to explore the resolution limit and imaging capabilities of XM-1.

Work continues to improve our existent cryogenic imaging system. This system allows imaging of biological specimens without prior chemical fixation that may affect cell structure, yielding more information about cells in a more natural state. It will also effectively eliminate beam damage to the cells. The addition of a calibrated tilt stage will allow tomographic three-dimensional reconstruction of a cell and quantitative assessment of protein localization.

## ACKNOWLEDGMENTS

The authors would like to thank the Department of Energy's Office of Basic Energy Sciences, DARPA, and the Air Force Office of Scientific Research for their generous support.

## REFERENCES

1. W. Meyer-Ilse, H. Medeck, L. Jochum, E. H. Anderson, D. Attwood, C. Magowan, R. Balhorn, M. Moronne, D. Rudolph, G. Schmahl, *Synchrotron Radiation News* **8**, pp. 23-33, 1995.
2. E. H. Anderson, D. L. Olynick, B. Harteneck, E. Veklerov, G. Denbeaux, W. Chao, A. Lucero, L. Johnson and D. Attwood Jr., "Nanofabrication and Diffractive Optics For High-Resolution X-Ray Applications," *J. Vac. Sci. Techn.*, 2000, in publication.
3. W. Chao, E. H. Anderson, G. Denbeaux, B. Harteneck, M. Le Gros, A. Lucero, D. Olynick, D. Attwood, "High Resolution Soft X-ray Microscopy," *SPIE* **4146**, 2000.
4. J. H. Underwood, E. M. Gullikon, "Beamline for measurements and characterization of multilayer optics for EUV Lithography," *SPIE* **3331**, p. 52.
5. G. Denbeaux, L. E. Johnson, W. Meyer-Ilse, "Spectromicroscopy at the XM-1," *X-Ray Microscopy*, Edited by W. Meyer-Ilse, T. Warwick and D. Attwood, pp. 478-483, AIP, New York, 1999.
6. P. Fisher, T. Eimüller and G. Schütz, "Element-Specific Imaging of Magnetic Domains at 25 nm Spatial Resolution Using Soft X-ray Microscopy," submitted to *Appl. Phys. Letters*.
7. B. W. Loo Jr., W. Meyer-Ilse and S. S. Rothman, "Automatic Image Acquisition, Calibration and Montage Assembly for Biological X-ray Microscopy," *J. Microscopy* **197**(2), pp. 185-201, 2000.
8. C. A. Larabell, D. Yager, W. Meyer-Ilse, "Localization of Proteins and Nucleic Acids Using Soft X-ray Microscopy," *X-Ray Microscopy*, Edited by W. Meyer-Ilse, T. Warwick and D. Attwood, pp. 107-112, AIP, New York, 2000.
9. W. Meyer-Ilse, D. Hamamoto, A. Nair, S. A. Lelièvre, G. Denbeaux, L. Johnson, A. Lucero, D. Yager, C. A. Larabell, "High Resolution Protein Localization Using Soft X-ray Microscopy," submitted to *J. of Microscopy*.